© 2018. Published by The Company of Biologists Ltd | Journal of Cell Science (2018) 131, jcs218123. doi:10.1242/jcs.218123

RESEARCH ARTICLE

Nuclear exclusion of SMAD2/3 in granulosa cells is associated with primordial follicle activation in the mouse ovary

Kate Hardy[1], Jocelyn M. Mora[1], Carina Dunlop[2], Raffaella Carzaniga[3,*], Stephen Franks[1,§] and Mark A. Fenwick[1,‡,§,¶]

ABSTRACT

Maintenance and activation of the limited supply of primordial follicles in the ovary are important determinants of reproductive lifespan. Currently, the molecular programme that maintains the primordial phenotype and the early events associated with follicle activation are not well defined. Here, we have systematically analysed these events using microscopy and detailed image analysis. Using the immature mouse ovary as a model, we demonstrate that the onset of granulosa cell (GC) proliferation results in increased packing density on the oocyte surface and consequent GC cuboidalization. These events precede oocyte growth and nuclear translocation of FOXO3a, a transcription factor important in follicle activation. Immunolabelling of the TGFβ signalling mediators and transcription factors SMAD2/3 revealed a striking expression pattern specific to GCs of small follicles. SMAD2/3 were expressed in the nuclei of primordial GCs but were mostly excluded in early growing follicles. In activated follicles, GC nuclei lacking SMAD2/3 generally expressed Ki67. These findings suggest that the first phenotypic changes during follicle activation are observed in GCs, and that TGFβ signalling is fundamental for regulating GC arrest and the onset of proliferation.

KEY WORDS: TGFβ, SMAD, Follicle, Primordial, Granulosa

INTRODUCTION

Female mammals are endowed with a finite complement of oocytes, which become enveloped by a single layer of flattened somatic granulosa cells (GCs) to form primordial follicles before or soon after birth (Edson et al., 2009). From the time of follicle formation, a steady trickle of follicles starts growing – a significant event in follicle development that defines reproductive lifespan. Throughout reproductive life, a diminishing population of primordial follicles are maintained in developmental arrest, and the factors maintaining this quiescence are unknown. Spatial analysis of primordial and growing follicles in sections of mouse ovary suggests that primordial follicles produce a local inhibitor that maintains them, and their close neighbours, in an arrested state (Da Silva-Buttkus et al., 2009).

[1]Department of Surgery and Cancer, Institute of Reproductive and Developmental Biology, Imperial College London, Hammersmith Hospital, Du Cane Road, London W12 0NN, UK. [2]Department of Mathematics, University of Surrey, Guildford GU2 7XH, UK. [3]Electron Microscopy Centre, Imperial College London, London SW7 2AZ, UK.
*Present address: The Francis Crick Institute, 1 Midland Road, London NW1 1AT, UK. ‡Present address: Academic Unit of Reproductive and Developmental Medicine, Department of Oncology and Metabolism, University of Sheffield, Level 4, The Jessop Wing, Tree Root Walk, Sheffield S10 2SF, UK.
§These authors contributed equally to this work

¶Author for correspondence (m.a.fenwick@sheffield.ac.uk)

M.A.F., 0000-0001-8856-2048

Received 23 March 2018; Accepted 31 July 2018

Activation of follicle growth involves changes in GC shape coupled with the onset of GC proliferation and oocyte growth (Adhikari and Liu, 2009; Da Silva-Buttkus et al., 2008; McGee and Hsueh, 2000; McLaughlin and McIver, 2009; Picton, 2001). The precise sequence of these events in the mouse and the identity of the activation factor remain unclear (Da Silva-Buttkus et al., 2008). These questions are important, as pinpointing which cell type (GCs or oocyte) and which cellular processes are the targets of this factor will help ascertain its identity and function.

Currently, the picture regarding the regulation of activation of follicle growth is incomplete. The use of mice carrying mutations in, or lacking, specific genes has identified key transcription factors and signalling pathways that play a role. In GCs, FOXL2 is reported to regulate early morphological changes (Schmidt et al., 2004; Uda et al., 2004) and key components of mTOR signalling have recently been associated with early proliferative events (Zhang et al., 2014). Transcription factors such as Sohlh1/2 (Choi et al., 2008), Nobox (Rajkovic et al., 2004), Lhx8 (Pangas et al., 2006), Foxo3a (Castrillon et al., 2003; Hosaka et al., 2004) and Ybx2 (Yang et al., 2005), as well as internal regulators of mTOR (Adhikari et al., 2009; Adhikari et al., 2010) and PI3K/Akt (Liu et al., 2006) signalling are also known to control early oocyte growth. Culture experiments using neonatal rat ovaries have identified possible candidate growth factors that stimulate activation of follicle growth *in vitro* (Skinner, 2005), and have confirmed the importance of kit ligand (KL) signalling in this process (Hutt et al., 2006; Nilsson and Skinner, 2004; Packer et al., 1994; Parrott and Skinner, 1999). One growth factor family that has attracted much attention is the TGFβ superfamily, with its downstream signalling molecules, the SMAD proteins (Knight and Glister, 2006; Pangas, 2012a,b). SMAD2 and SMAD3 (hereafter SMAD2/3) signalling is of particular interest due to their predominant expression in GCs of primordial and early growing follicles (Billiar et al., 2004; Drummond et al., 2002; Fenwick et al., 2013; Sharum et al., 2017; Xu et al., 2002). TGFβ signalling is an important regulator of cell proliferation (Massagué, 2012); however, the precise relationship between this signalling pathway and the early phenotypic changes in GCs of small follicles have not yet been examined.

The study of activation of follicle growth is problematic. Many knockout mouse models are embryonic lethal, and conditional knockouts created to study follicle development use promoters for genes whose expression is amplified after follicles start to grow, such as AMHR2, ZP3 or GDF9. Furthermore, primordial and transitional follicles are difficult to isolate because of their small size (up to 20 µm) and fragility, and they fail to thrive *in vitro* and provide scant amounts of mRNA and protein for analysis. Conventional GC culture approaches are not useful as they involve the use of GCs aspirated from antral follicles, which differ from flattened cells in primordial follicles in terms of phenotype, hormone and growth factor production and responsiveness, and gene expression patterns

Journal of Cell Science (2018) 131, jcs218123. doi:10.1242/jcs.218123

(Herrera et al., 2005; Liu et al., 2001; Mora et al., 2012). We therefore chose to investigate follicle activation *in situ*, in the freshly dissected intact ovary, which maintains the three-dimensional environment that is essential for the health of these very small follicles, as well as allowing precise identification of morphological changes associated with activation of follicle growth.

In this study, our key objectives were to identify which follicle cell type initially undergoes morphological changes as follicles activate and determine how these changes relate to indicators of TGFβ signalling. We used immunohistochemistry and image analysis to carry out systematic measurements of follicle and oocyte growth, GC proliferation and shape change. We demonstrate that GC proliferation is associated with a subtle but clear change in GC shape which precedes the formation of cuboidal cells, suggesting that cuboidalization is an event resulting from increased packing density of GCs on the oocyte surface. Furthermore, we show that these GC-based events occur before the oocyte starts growing. We have gone on to localize and quantify nuclear and cytoplasmic SMAD2/3 in the GCs of primordial and activating follicles and show that loss of nuclear SMAD2/3 is associated with the onset of GC proliferation. This has allowed us to propose that the GCs are a target for the activating signal and that upstream inhibitory factors of the TGFβ-SMAD2/3 pathway are likely candidates for regulating activation of follicle growth.

RESULTS

A new morphological stage for follicles initiating growth

Primordial follicles are surrounded by a few flattened granulosa cells (Fig. 1A,E,I), whereas primary follicles are enveloped in a single layer of cuboidal cells (Fig. 1D,H,L). In our earlier studies we used the term ‘transitional follicle’ to describe follicles that are intermediate between primordial and primary stages and which

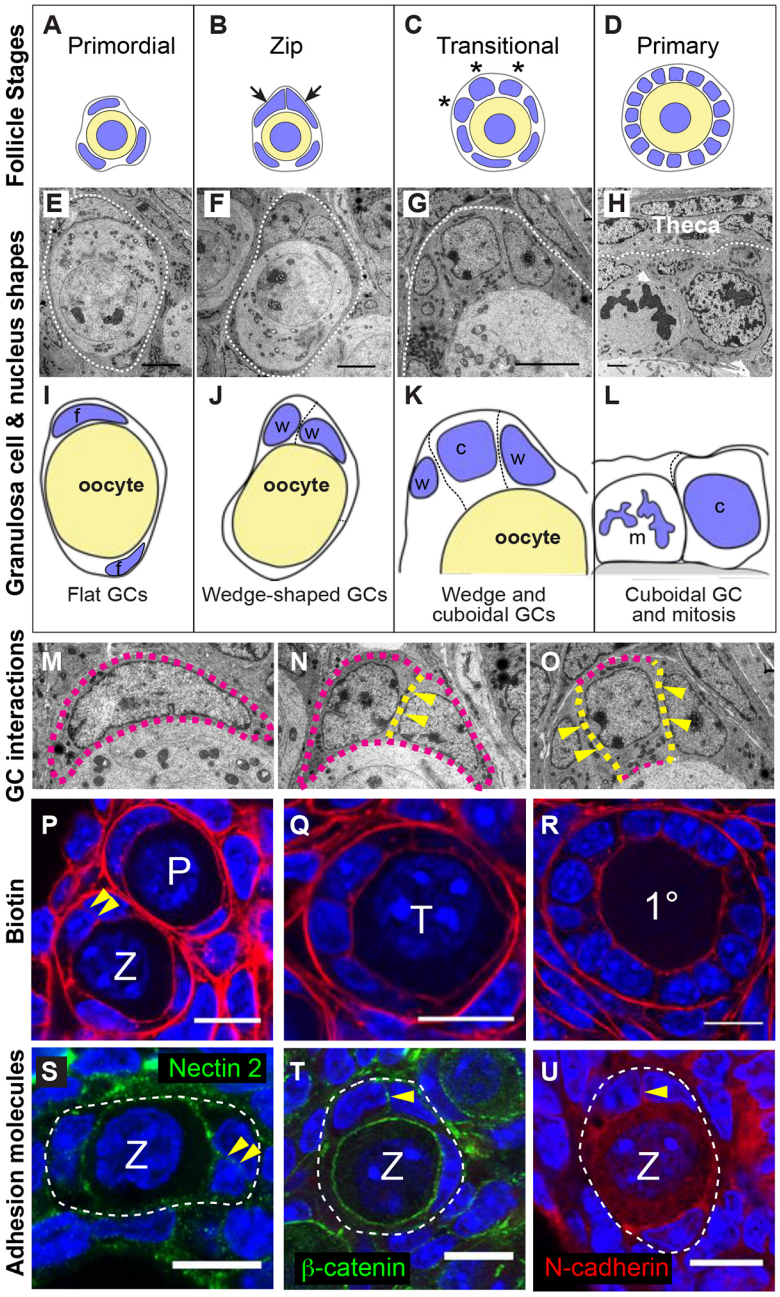

Fig. 1. Morphological changes in GCs during activation of follicle growth. Line drawings (A-D), electron micrographs (E-H) and line tracings of electron micrographs (I-L) showing changes in granulosa cell shape during the earliest stages of preantral follicle development. (A-D) GC and oocyte nuclei in blue and ooplasm in yellow. The primordial follicle is enveloped in flattened GCs (A,E,I). The ‘zip’ follicle shows the development of two wedge-shaped GC cells (arrows in B), which have an extended interface between the neighbouring GCs (B,F,J; arrowheads in N). At the transitional stage, cuboidal cells (asterisks in C and cell labelled ‘c’ in K) develop (C,G,K). The oocyte in the primary follicle is completely enclosed by cuboidal cells (D,H,L). (E-H, see I-L for annotations) Electron micrographs showing the ultrastructure of (E) a primordial follicle with two flattened GCs (f); (F) a zip follicle with two wedge-shaped cells (w); (G) a transitional follicle with a cuboidal (c) and two wedge-shaped cells (w); (H) a primary follicle with a cuboidal cell (c) and a cell in mitosis (m). White dotted lines show basal lamina. (I-L) Line drawings highlighting the key features of GC and nuclear shape and cell boundaries in the EM images. Scale bars: 10 µm (E-G), 2 µm (H). Images in F and N were originally published in fig. 7 of Mora et al. (2012).(M-O) Magnification of GCs in (E-G) showing development of extended intercellular contacts between adjacent GCs (yellow dotted lines, arrowed). Pink dotted line marks outline of GCs. (P-R) Follicles at successive stages with cell membranes labelled with biotin (red) as described previously (Mora et al., 2012) and nuclei with DAPI (blue). Extended intercellular contact in zip follicle indicated by arrowheads. (S-U) Onset of expression of adhesion or adhesion-associated molecules in extended contacts (arrowheads) between adjacent GCs in zip follicles, including nectin 2 (green, S), β-catenin (green, T) and N-cadherin (red, U). Scale bars: 10 µm.

Journal of Cell Science (2018) 131, jcs218123. doi:10.1242/jcs.218123

are surrounded by a mixture of flattened and cuboidal cells (Fig. 1C, G,K) (Da Silva-Buttkus et al., 2008; Mora et al., 2012; Stubbs et al., 2007). Previously, careful measurement of transitional follicles showed that they had more GCs and larger oocytes than primordial follicles, and it was difficult to show with precision which event occurred first, oocyte growth or GC proliferation (Da Silva-Buttkus et al., 2008). Further experience of follicle morphology and granulosa cell adhesion allowed us to identify a new intermediate stage between primordial and transitional, where two adjacent granulosa cells had formed wedge shapes with an elongating contact between them (Mora et al., 2012). Their appearance was suggestive of the first division of a flat cell (Fig. 1M) into two adjacent daughter cells (Fig. 1N); we descriptively named these 'zip' follicles, as they showed granulosa cell contacts that were 'zipping up' and lengthening (Fig. 1B,F,J). The key feature of a zip follicle is that it exhibits the first substantial region of adhesion between two adjacent granulosa cells (Fig. 1N) which extends perpendicular to the oocyte surface, i.e. it is the first phenotypic sign of the onset of change in shape of GCs leading to cuboidalization (Fig. 1O). Retrospective analysis of images of early pre-antral follicles acquired during our previous study (Mora et al., 2012) showed the changes in GC shape (Fig. 1P-R) and expression of the adhesion molecules N-cadherin and nectin 2, as well as the adhesion-related protein β-catenin in the extending interface between the two adjacent GCs (Fig. 1S-U). These follicles became our focus for further study.

GCs proliferate and change shape before the oocyte grows

The boundary of follicles is not always clear in sections of ovary stained with the nuclear stain DAPI. Therefore, double immunofluorescence for basal lamina-specific laminin and oocyte-specific DDX4 with a DAPI counterstain was carried out to clearly define the basal lamina surrounding the follicle, the oocyte and oocyte nucleus, respectively (Fig. 2A), allowing accurate measurement of their area. Only follicles where the oocyte had a pure blue nucleus with a clear outline were measured, to ensure that the follicle was at its largest cross section (LCS) (Fig. 2B). Follicles with an indistinct basal lamina or which were lying in the ovarian surface epithelium (OSE; outside the OSE basal lamina) were excluded (Fig. 2A). Using ImageJ, measurements of the area of the follicle, oocyte and oocyte nucleus were made, and the number of GC nuclei visible in the image was counted (Fig. 2C). Mean GC height, area and width were calculated from these values.

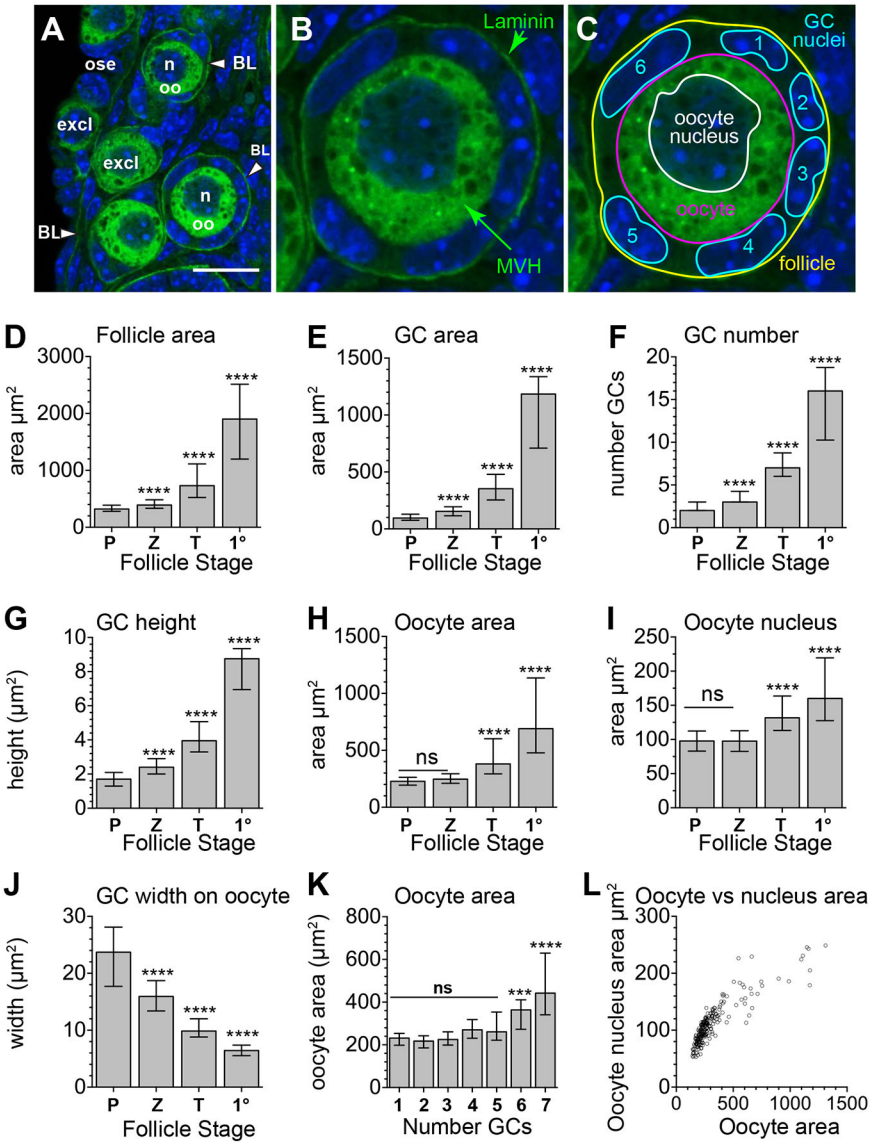

Fig. 2. Comparison of follicle, oocyte and GC area as follicles develop. (A,B) Immunofluorescence localization of laminin (BL, green) and MVH (oo, green) to clearly delineate the boundary of the follicle and oocyte for accurate measurement. Cell nuclei are labelled with DAPI (blue). Three 5-µm-thick sections from each of three d12 ovaries were analysed (243 unilaminar follicles in total). Note the lack of a basal lamina in follicles lying in the ovarian surface epithelium (ose). Scale bars: 10 µm. excl, excluded from analysis; n, oocyte nucleus; oo, oocyte; BL, basal lamina. (C) Diagram showing follicle measurements made using ImageJ, including follicle area (yellow line), oocyte area (pink line), oocyte nucleus area (white line). The number of DAPI-stained GC nuclei (delineated by turquoise lines) were counted (six in this example). GC area=follicle area−oocyte area; GC height=(follicle diameter−oocyte diameter)/2; GC width=number of GC nuclei/oocyte circumference. (D) Follicle area. (E) GC area. (F) Number of DAPI-labelled GC nuclei in largest cross section (LCS). (G) GC height. (H) Oocyte area. (I) Oocyte nucleus area. (J) GC width. (K) Oocyte area compared with number of GCs in the LCS. Note lack of significant oocyte growth between one and five GCs. (L) Relationship between oocyte area and oocyte nucleus area. (D-K) Bars are median±interquartile range. Results are compared with primordial stage using Kruskal-Wallis test with Dunn's multiple comparisons post test. ***P<0.001, ****P<0.0001; ns, not significant.

Journal of Cell Science (2018) 131, jcs218123. doi:10.1242/jcs.218123

The area of zip follicles was significantly larger than that of primordial follicles (Fig. 2D). The increased follicle area was due to an increased GC area (Fig. 2E), number of GCs (Fig. 2F) and GC height (Fig. 2G), but not to a larger oocyte (Fig. 2H). Of critical importance, the oocytes (and the oocyte nuclei) in zip follicles were the same size as in primordial follicles (Fig. 2H,I). The combination of increased GC number with the absence of oocyte growth resulted in a higher packing density of GCs on the oocyte surface (Fig. 2J). If we go on to compare oocyte area to the number of GCs seen in the LCS, we see that there is no significant oocyte growth until there are six or more GCs in the LCS (Fig. 2K). Interestingly, in the earliest stages of follicle growth, the oocyte nucleus grows as the oocyte grows, reaching a maximal size as the oocyte exceeds an area of ~500 µm^2 (a diameter of ~25 µm, Fig. 2L).

These data indicate that the GCs start to proliferate and change shape before the onset of oocyte growth, suggesting that, in the mouse, the GCs are the first cells to respond, at least in terms of morphology, to an activation signal. Previously, we had considered that the response to such a signal could be a change in cell shape followed by GC proliferation (Da Silva-Buttkus et al., 2008; Mora et al., 2012). However, the current data led us to consider the alternative scenario that, in response to the unknown signal, flat GCs start to occasionally proliferate and become more packed on the oocyte surface, resulting in an increase in GC height and cuboidalization, as we observed (Fig. 2G).

Proliferation increases in 'zip' follicles

The increased number of GCs in zip follicles prompted us to quantify granulosa cell proliferation at the primordial, zip, transitional and primary stages. Ki67 is generally accepted to be an accurate marker of cell proliferation, particularly in cells undergoing rapid proliferation such as cell lines and malignant cells. However, Ki67 labelling in primordial follicles is rare in both mouse and human (Da Silva-Buttkus et al., 2008; Stubbs et al., 2007) because of the infrequency of cell division, so we chose to use the proliferation marker PCNA, which has been used previously in studies on GC proliferation (Gougeon and Busso, 2000; Lundy et al., 1999; Oktay et al., 1995; Wandji et al., 1997; Wandji et al., 1996). PCNA has a longer half-life of ~20 h (Bravo and Macdonald-Bravo, 1987), compared with ~1 h for Ki67 (Scholzen and Gerdes, 2000), so label persists longer after S phase or after cells have re-entered G_0. It is therefore possible to detect GCs that are in the process of, or have recently undergone, cell division in cells with a low proliferation rate.

The proportion of zip follicles with one or more PCNA-positive GCs (Fig. 3A-C) was significantly higher than that in primordial follicles (Fig. 3D). Similarly, the proportion of PCNA-positive GCs per follicle was significantly higher in zip follicles than in primordial follicles (Fig. 3E). We confirmed our findings with a second marker of proliferation, minichromosome maintenance protein 2 (MCM2; Fig. 3F-J), which we have previously used to examine GC proliferation in human GCs (Stubbs et al., 2007). These observations support the concept that the zip phenotype is associated with increased GC proliferation and accompanying change in cell shape, and the hypothesis that GCs are the first cell type to respond phenotypically to an unknown activation signal.

FOXO3 exclusion from the oocyte nucleus occurs after the onset of GC proliferation

We have shown that the onset of GC proliferation occurs before that of oocyte growth. We recognise that the oocyte is a metabolically active cell and that morphological changes are likely to occur

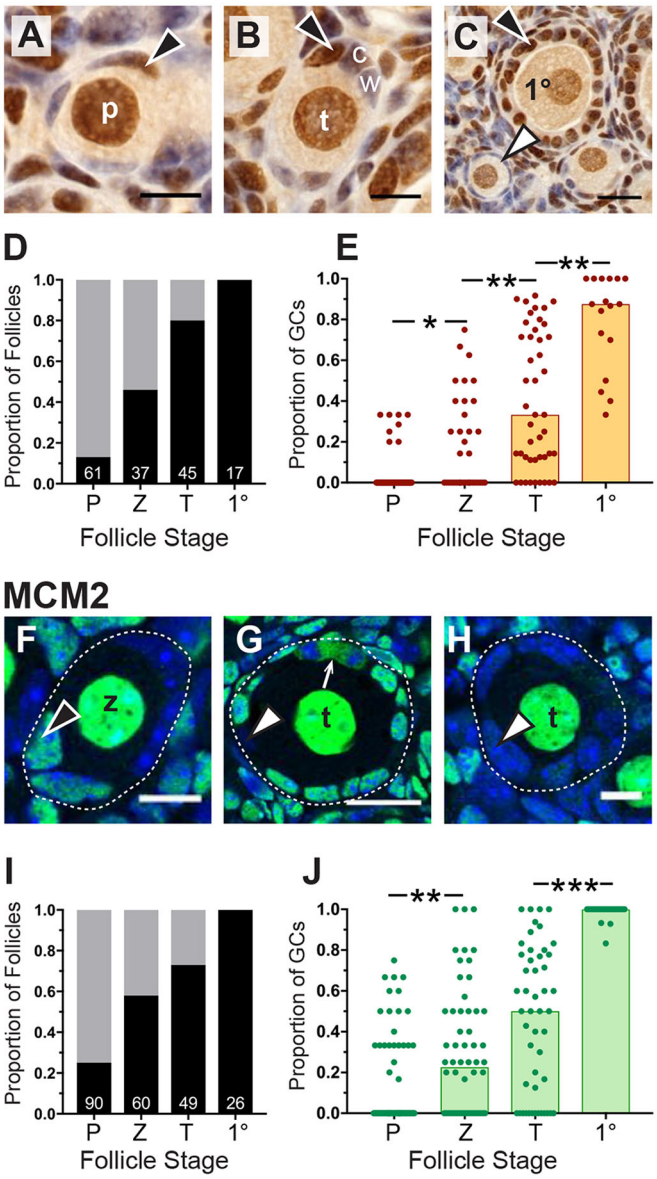

Fig. 3. Quantification of GC proliferation using PCNA and MCM2. Two to three sections from each of three d12 ovaries were immunolabelled for the proliferation marker PCNA or MCM2, and the number of positive and negative GCs counted in 160 follicles for each marker. PCNA-positive nuclei (black arrowheads) in primordial (A), transitional (B) and primary (C) follicles; P, primordial; t, transitional; 1°, primary; w, wedge-shaped GC; c, cuboidal GC. Scale bars: 10 µm. Note the PCNA-negative follicle (white arrowhead) indicating that all the flat GCs are in G0 of the cell cycle at this particular time point. (D) Proportion of follicles with one or more PCNA-positive GCs (black bars), or no positive GCs (grey bars). Proportions are significantly different (Chi-squared test, $P<0.0001$, with a significant trend). (E) Proportion of PCNA-positive GCs at each follicle stage. Bars are medians, sequential stages were compared using Kruskal-Wallis test with Dunn's multiple comparisons post test; *$P<0.05$, **$P<0.01$. (F-H) MCM2-positive nuclei (green, black arrowhead) in a zip follicle (z; F). Note the lateral mitosis (white arrow), and unlabelled GC (white arrowhead; G). (H) No labelling in a transitional follicle (white arrowhead), demonstrating how GCs can enter and leave the cell cycle even after activation. Scale bars: 10 µm (F,H) and 20 µm (G). (I) Proportion of follicles with one or more MCM2-positive GCs (black bars) or no positive GCs (grey bars). Proportions were significantly different (Chi squared $P<0.0001$, with a significant trend). (J) Proportion of MCM2-positive GCs at each follicle stage. Bars indicate medians and results are compared as above; **$P<0.01$, ***$P<0.001$. Number of follicles analysed for each stage is indicated in D and I. P, primordial; Z, zip; T, transitional; 1°, primary.

Journal of Cell Science (2018) 131, jcs218123. doi:10.1242/jcs.218123

following internal molecular events. Therefore, we wanted further evidence to support the hypothesis that the GCs, rather than the oocyte, are the first to undergo phenotypic changes. FOXO3 is a transcription factor that is expressed in oocyte nuclei and undergoes nuclear exclusion as follicles activate growth (Fig. 4A). This is a well-documented event that is linked to PI3K signalling (John et al., 2008; Liu et al., 2007a), but the precise stage at which this occurs has not been previously quantified.

The intensity of FOXO3A staining was quantified in greyscale images (Fig. 4B,C). There was no difference in oocyte nucleus FOXO3 intensity between primordial and zip follicles. Transitional and primary oocyte nuclei had significantly less staining (Fig. 4D). Ooplasmic FOXO3 intensity remained constant in follicles from the primordial to the primary stage (i.e. as they activated growth; Fig. 4E). In a further analysis aimed at controlling for variability in staining intensity between follicles, sections and ovaries, the difference between nuclear and cytoplasmic FOXO3 intensity within each oocyte was calculated and compared. The difference between nuclear and cytoplasmic intensity was similar in primordial and zip follicles, was significantly less marked in transitional follicles, while in primary follicles the nucleus was lighter than the cytoplasm (Fig. 4F).

Next, we wanted to compare both intensity of nuclear FOXO3 in oocytes and onset of GC proliferation with oocyte growth. GC proliferation occurred before nuclear FOXO3A exclusion in the oocyte growth trajectory. A significant increase in GC number was observed in oocytes that were 20 and 25 µm in diameter, whereas significant FOXO3A exclusion was seen when oocytes were between 30 and 35 µm in diameter (Fig. S1A), when follicles are reaching the primary stage and starting to multilayer (Fig. S1B). This further supports our argument that GC behaviour changes first.

SMAD2/3 labelling decreases as follicles develop

As the TGFβ superfamily is the major group of growth factors involved in follicle development (Knight and Glister, 2006; Pangas, 2012b), and SMAD2/3 is strongly expressed in primordial and early growing follicles (Billiar et al., 2004; Drummond et al., 2002; Fenwick et al., 2013; Sharum et al., 2017; Xu et al., 2002) we went on to quantify and localize SMAD2/3 during activation of follicle growth. SMAD 2/3 was expressed in the GCs, but not in the oocyte (Fig. 5A-D). Upon inspection, it became clear that some nuclei were SMAD2/3 positive, whereas others were negative. SMADs are known to shuttle between the cytoplasm and nucleus under both basal and stimulated conditions; however, increased nuclear dwell time is a feature of active SMAD signalling (Hill, 2009). This prompted us to examine the expression of nuclear SMAD in more detail in individual follicles. To quantify nuclear and cytoplasmic SMAD, we applied a set threshold to the green (SMAD) channel. Using a sampling circle of fixed pixel diameter, we measured the proportion of pixels exceeding the threshold in nuclei and in a neighbouring area of cytoplasm (Fig. 5E). This approach clearly showed that there were nuclei that had negligible levels of SMAD (Fig. 5A′ to D′,E, white arrows). The majority of nuclei in primordial follicles were SMAD2/3 positive, but the proportion of nuclei lacking SMAD2/3 (or with negligible levels), increased as follicle development progressed ($P \leq 0.0001$, Chi-square test for trend; Fig. 5F). The key observation was that there was a significant increase in the proportion of SMAD2/3-negative nuclei (with <1% positive pixels) in zip follicles compared with primordial follicles ($P=0.0021$, Fisher's Exact test; Fig. 5G).

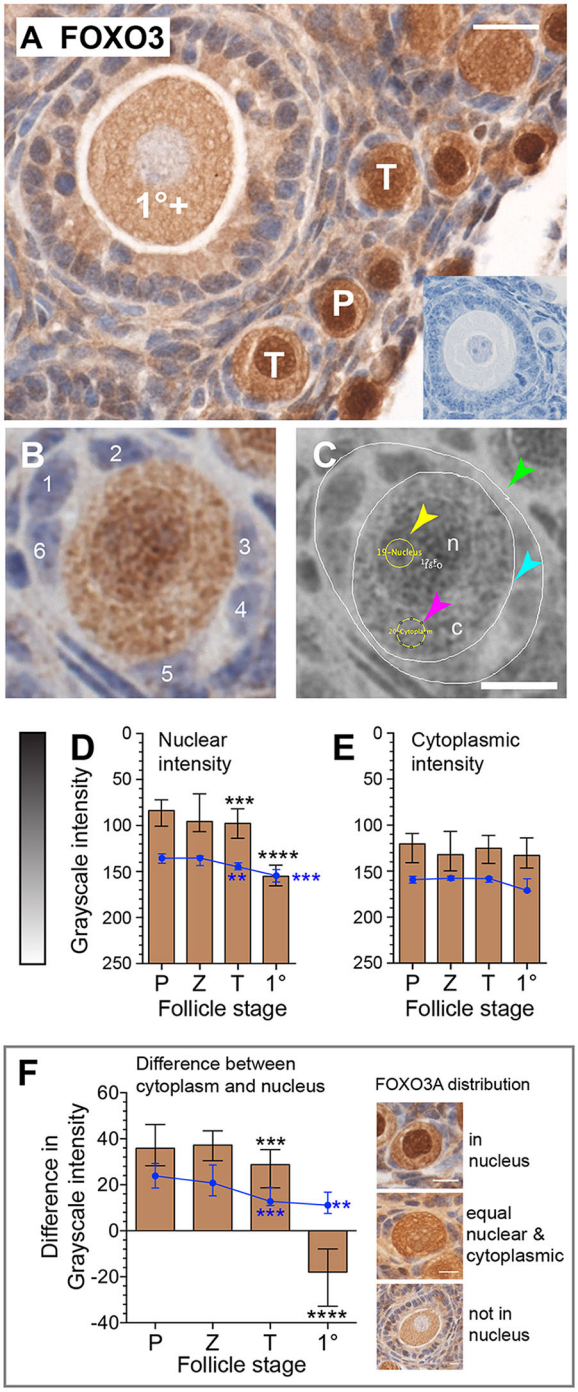

Fig. 4. FOXO3 export from oocyte nuclei during activation of follicle growth. FOXO3 expression (brown) was measured in 267 follicles in two to three sections from three ovaries (A). Seventy haematoxylin-only (blue) control follicles were also analysed (A, inset). (B) For each follicle, stage and number of GCs was recorded. (C) Screenshot of an ImageJ analysis of FOXO3a intensity in a transitional follicle. In the greyscale image (0=black, 255=white), a sampling circle of constant pixel size was used to measure FOXO3a intensity in the oocyte nucleus (n, yellow arrow) and cytoplasm (c, pink arrow). In addition, follicle (green arrow) and oocyte (turquoise arrow) area was measured. (D,E) Nuclear (D) and cytoplasmic (E) intensity in follicles at progressive stages. Brown bars, FOXO intensity; blue line, intensity of haematoxylin alone. (F) Difference in intensity between nucleus and cytoplasm. Bars and lines in D-F are median ±interquartile range. Results are compared to primordial stage using Kruskal-Wallis test with Dunn's multiple comparisons post test; **$P<0.01$, ***$P<0.001$, ****$P<0.0001$. P, primordial; Z, zip; T, transitional; 1°, primary; 1°+, primary follicle with second layer of GCs appearing.

Journal of Cell Science (2018) 131, jcs218123. doi:10.1242/jcs.218123

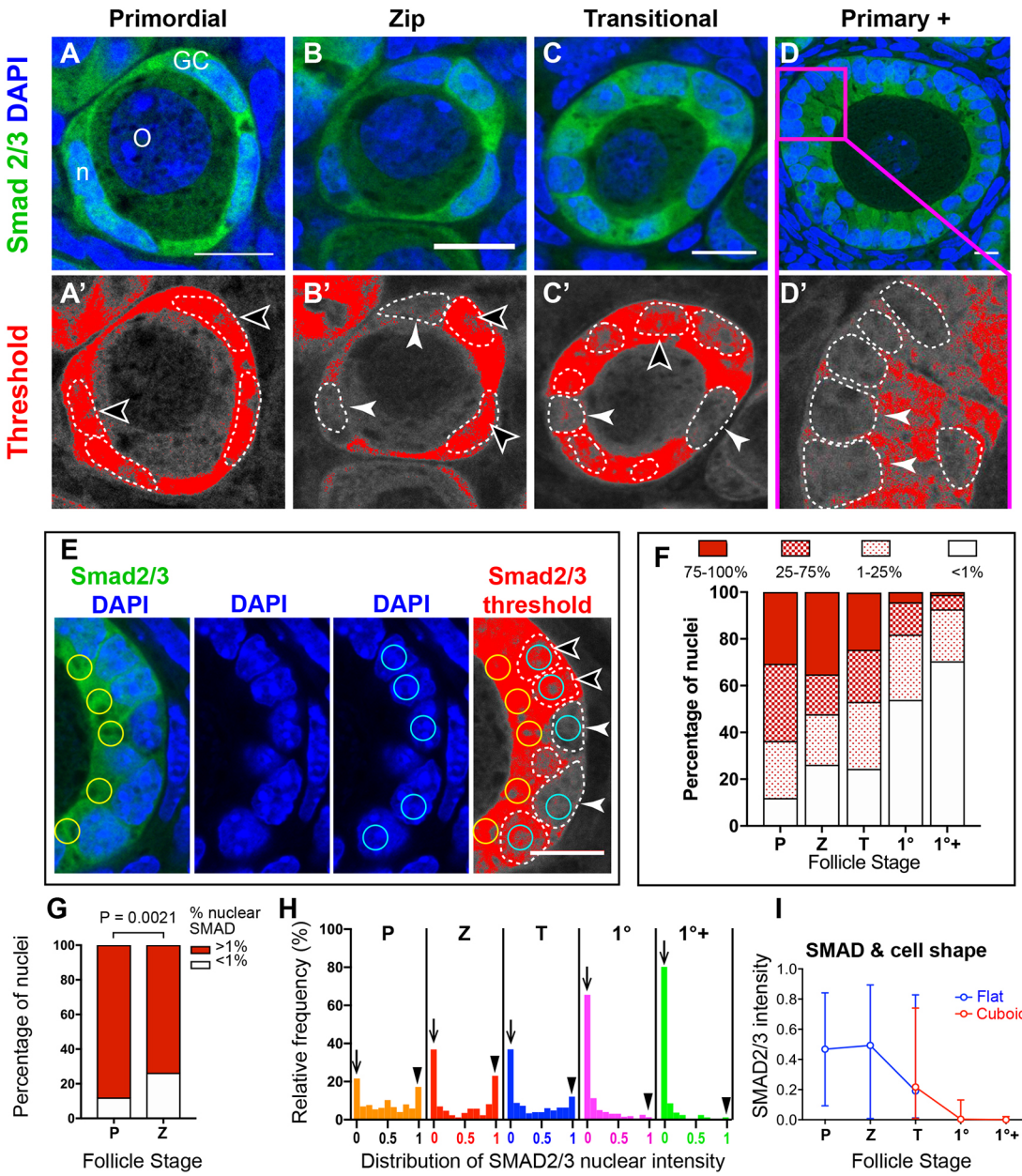

Fig. 5. SMAD2/3 expression during activation of follicle growth. SMAD2/3 expression was examined in 1090 GCs in 246 follicles from primordial to primary plus stages. Primordial (A), zip (B), transitional (C) and primary+ (D) follicles labelled for SMAD2/3 (green) and DAPI (blue). (A′-D′) Greyscale image (ImageJ) of the green channel (SMAD2/3) showing pixels above a set threshold to indicate positive staining (red). Dotted lines delineate GC nuclei. White arrows indicate SMAD-negative nuclei, black arrows show SMAD-positive nuclei. (E) A sampling circle of consistent pixel area was used to measure the area of SMAD2/3-positive pixels over a set threshold in 1-20 GC nuclei per follicle [turquoise circles, positioned in the blue (DAPI) channel] and adjacent regions of cytoplasm [yellow circles, positioned in the green (SMAD) channel of an RGB stack]. (F) Percentage of nuclei with negligible (<1%), low (1-24.9%), moderate (25-74.9%) or high (75-100%) percentages of SMAD2/3-positive pixels at different follicle stages. There is a significant change in the percentage of nuclei with different levels of SMAD positivity, $P<0.0001$, Chi-square test for trend. (G) Percentage of GC nuclei with negligible nuclear SMAD (<1%) was significantly lower in primordial follicles compared with zip follicles (Fisher's Exact test). (H) Distribution of the percentage of GC nuclei with an increasing proportion of positive pixels in GC at progressive stages of follicle development. The proportion of positive pixels in nuclei ranges from 0 (no positive pixels, arrow) to 0.1, 0.2, 0.3 etc. to 1 (where all pixels are positive, arrowhead). (I) Effect of cell shape on nuclear SMAD2/3. Values are median±interquartile range of the points. Scale bars: 10 µm. P, primordial; Z, zip; T, transitional; 1°, primary; 1°+, primary plus.

We went on to examine how follicle stage affected the distribution of nuclei with negligible (Fig. 5H, arrow), intermediate and high (Fig. 5H, arrowhead) intensity of nuclear SMAD2/3. Primordial and zip follicles had nuclei with either negligible or very high levels of SMAD2/3, as shown by the peaks at either end of the distribution, as well as intermediate levels. As development progressed, an increasing percentage of follicles had negligible SMAD2/3 (Fig. 5H, arrows), with a decreasing percentage having very high levels (Fig. 5H, arrowheads). Finally, we examined whether there was a relationship between nuclear intensity of SMAD and the shape of the GC and showed that flat GCs had higher levels of SMAD2/3 than cuboidal GCs (Fig. 5I). Interestingly, total SMAD levels in the GC layer,

Journal of Cell Science (2018) 131, jcs218123. doi:10.1242/jcs.218123

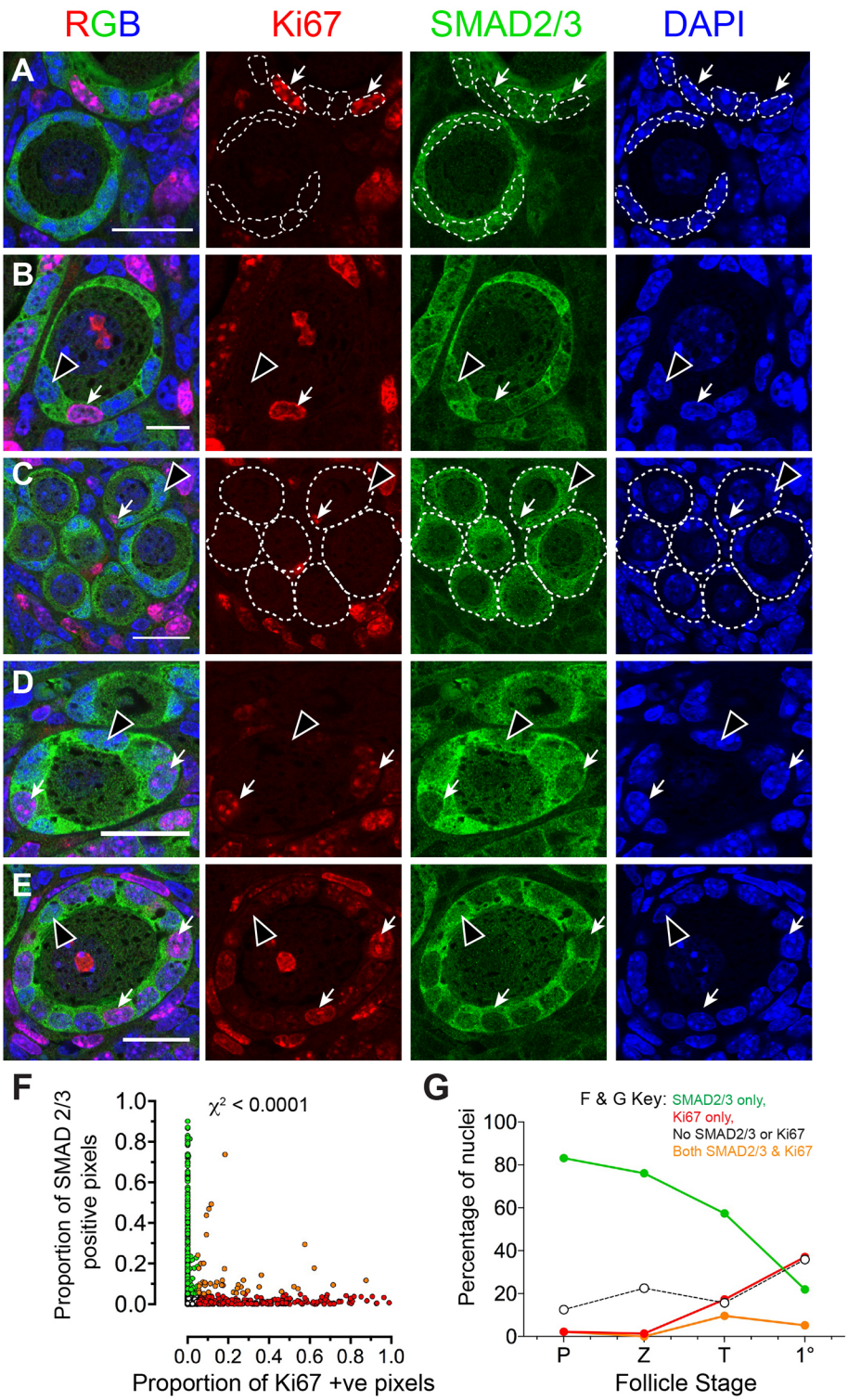

Fig. 6. Nuclear SMAD2/3 and proliferation. Double immunofluorescence of Ki67 and SMAD2/3. Three sections, each from a different d12 ovary, underwent double immunofluorescence labelling for SMAD2/3 and the proliferation marker, Ki67. A total of 828 clearly delineated nuclei were analysed in primordial (*n*=72), zip (*n*=26), transitional (*n*=34) and primary (*n*=37) follicles. The area of SMAD2/3- or Ki67-positive pixels was calculated as a proportion of the area of the nucleus. Lack of Ki67 or SMAD2/3 labelling was defined as a proportion of positive pixels of <0.05. (A,B) Unilaminar follicles immunolabelled for Ki67 (red) and SMAD2/3 (green) showing nuclei (blue, DAPI) that are positive for Ki67 and negative for SMAD2/3 (white arrows) and conversely negative for Ki67 and positive for SMAD2/3 (black arrowhead). White dotted lines in A delineate nuclei. (C) Cluster of primordial follicles showing all nuclei negative for Ki67 and positive for SMAD2/3, with the exception of one (white arrow). White dotted lines delineate follicles. (D) Transitional follicle with two Ki67-positive nuclei with minimal nuclear SMAD2/3 (white arrows). (E) Primary follicle with the majority of nuclei lacking SMAD2/3, with varying levels of Ki67. Two nuclei (white arrows) have minimal SMAD2/3 and strong Ki67 positivity. One nucleus (black arrowhead) is SMAD2/3 positive and lacks Ki67. (F) Proportion of positive pixels for SMAD2/3 and Ki67 measured in individual nuclei. (G) Percentage of nuclei positive or negative for Ki67 and/or SMAD2/3 at progressive stages of follicle development. P, primordial; Z, zip; T, transitional and 1°, primary. Scale bars: 20 µm.

including both nuclear and cytoplasmic expression, declined with follicle stage, especially from the primary stage onwards (Fig. S2).

In summary, primordial follicles have the highest proportion of SMAD2/3-positive nuclei, suggesting that signalling through the SMAD2/3 pathway may play a role in the maintenance of the primordial pool. A similar pattern of SMAD2/3 expression in early stage follicles from adult mouse ovaries was also seen, confirming that the findings were not exclusively related to the immature ovary (Fig. S3).

Nuclear localization of SMAD2/3 disappears with GC proliferation

The variability of nuclear SMAD2/3 expression in primordial, zip and transitional follicles, and the presence of increasing numbers of nuclei totally lacking SMAD2/3 as development progressed, led us to ask whether there was an association between nuclear SMAD expression and GC proliferation. For this, we used a cell cycle marker with a shorter half-life, Ki67, to get an accurate snapshot in time of proliferation and nuclear SMAD2/3 occupancy. Sections

Journal of Cell Science (2018) 131, jcs218123. doi:10.1242/jcs.218123

from three ovaries were examined, encompassing 169 follicles with a total of 828 nuclei (Table S1). The key finding was that expression of SMAD2/3 and Ki67 was mutually exclusive in the majority of nuclei, with Ki67 expression occurring predominantly in nuclei lacking SMAD2/3 (Fig. 6A-E, white arrows). Of the GCs lacking nuclear SMAD2/3, 47% were positive for Ki67. Conversely, 82% of Ki67-positive GCs were negative for SMAD2/3. Only a small proportion (5%) of GC nuclei contained both SMAD2/3 and Ki67 (Fig. 6F). Each ovary demonstrated a similar expression pattern (Fig. S4). As follicles progressed through development, the percentage of SMAD2/3-positive nuclei declined, whereas the percentage of Ki67-positive nuclei increased (Fig. 6G).

The expression of Ki67 in nuclei lacking SMAD2/3 led us to conclude that this signalling pathway is associated with the maintenance of GCs in cell cycle arrest, and furthermore, that the onset of GC proliferation is associated with the exclusion of SMAD2/3 from the nucleus.

DISCUSSION

Here, we have shown that as follicles activate, GC proliferation precedes phenotypic changes in the oocyte, including growth of the oocyte and its nucleus, and FOXO3 export from the oocyte nucleus. Furthermore, we have shown that the canonical TGFβ signalling mediators and transcription factors SMAD2/3 are expressed in the nuclei (>80%) of primordial GCs, suggesting that this pathway is involved in inhibition of GC proliferation and maintenance of the primordial pool. We have previously proposed that primordial follicles themselves produce a local inhibitor that prevents activation of follicle growth, and that follicles only start to grow in regions where levels of this putative, and as yet unidentified, inhibitor are reduced (Da Silva-Buttkus et al., 2009). The data presented here indicate that the putative inhibitor is likely to be a member of the TGFβ superfamily that signals via the SMAD2/3 pathway. Moreover, as follicles begin to grow, the loss of nuclear SMAD2/3 in GCs indicates that perturbation of this signalling pathway is a key molecular event associated with further proliferation and differentiation.

Key spatial information is lost when whole ovaries are homogenized for standard RNA or protein techniques. Therefore, identifying the genes associated with the primordial phenotype and the molecular changes that occur as follicles activate requires detailed image analyses. Based on the morphometric analyses in this study, as follicles activate, GCs initially proliferate and subsequently change shape. This is consistent with reports in other species that have also suggested that changes in GCs precede oocyte enlargement during follicle activation (Braw-Tal, 2002; Hirshfield, 1991; Lintern-Moore and Moore, 1979; Stubbs et al., 2007). Importantly, the observed change in shape is likely to occur as a consequence of an increased number of GCs occupying the surface of the oocyte. GCs of single-layered follicles are tethered basally to the basal lamina via hemidesmosomes (Da Silva-Buttkus et al., 2008) and apically to the oocyte via strong heterotypic N-cadherin–E-cadherin and Nectin-2–Nectin-3 adherens junctions (Mora et al., 2012). The latter attachments are strong and cannot be disrupted even in Ca^{2+}-free conditions. Flat cells have little intercellular contact with each other, but a large area of contact with the oocyte, which has a finite surface area. As the GCs divide parallel to the oocyte surface (see Fig. 3G, arrow, for an example), their contact area with the oocyte decreases. Following division, the daughter cells become abutted to each other, forming two wedge-shaped cells with an increased area of lateral contact between them, which start to express Nectin 2 and N-cadherin, characteristic of adherens junctions (Mora et al., 2012), (Fig. 1). Adherens junctions play a role in both intercellular adhesion and intracellular signalling (Andl and Rustgi, 2005; Erez et al., 2005). The increased intercellular contact and expression of adherens junctions as GCs divide, become more packed and change shape, may lead to increased intracellular signalling from these junctions, further stimulating GC proliferation. This could explain our previous observation that cuboidal cells proliferate more than flat cells (Da Silva-Buttkus et al., 2008).

Recent advances in stem cell technologies have made it possible to derive oocyte-somatic cell complexes and recapitulate follicle development *in vitro* (Hikabe et al., 2016). Despite this advance, it has not yet been possible to produce true primordial follicles *in vitro*, partly due to a lack of molecular details associated with the pre-granulosa cell phenotype. In this report, we have used high-resolution confocal imaging to analyse the sub-cellular expression of SMAD2/3. The general localization of SMAD2/3 is consistent with previous studies indicating that SMAD2/3 is predominantly expressed in GCs of small (single and multi-layered) pre-antral follicles (Fenwick et al., 2013; Sharum et al., 2017; Xu et al., 2002). Although the antibody used in this study does not discriminate phosphorylated from non-phosphorylated forms, the expression of these transcription factors in the nuclei of GCs of primordial-transitional follicles implies that this signalling pathway is actively regulating genes in these cells. TGFβ signalling is known to regulate a variety of cellular responses depending on the context, and in epithelial cells is often associated with maintaining a cytostatic phenotype (Massagué, 2012; Zhang et al., 2017). Since GCs from single-layered follicles are typically characterized as having low rates of proliferation, with some ‘epithelial-like’ qualities, including expression of cytokeratin and attachment to a basal lamina (Da Silva-Buttkus et al., 2008; Mora et al., 2012), we propose a role for TGFβ signalling in this context.

Previous spatial analysis has proposed the existence of a locally produced inhibitory factor (Da Silva-Buttkus et al., 2009), which we now believe to be a TGFβ family member. Candidate ligands known to activate SMAD2/3 include TGFβ-1, -2, -3, activins, nodal and several members of the growth differentiation factor (GDF) sub-family (Wakefield and Hill, 2013). Binding of the ligand to type I and II TGFβ receptors results in phosphorylation of SMAD2/3, which promotes their translocation to the nucleus to form transcriptional complexes to regulate target genes (Massagué, 2012). In epithelial cells, these complexes can regulate the expression of genes involved in the cell cycle, including *Myc* and the CDK inhibitors *Cdkn1a*, *Cdkn1b* and *Cdkn2b* (which encode $p21^{CIP1}$, $p27^{KIP1}$ and $p15^{INK4B}$, respectively) (Chen et al., 2002; Frederick et al., 2004; Hannon and Beach, 1994; Lecanda et al., 2009; Seoane et al., 2001). Interestingly, $p27^{KIP1}$ is expressed in primordial GCs and deletion of $p27^{KIP1}$ in mice causes premature activation of follicles (Rajareddy et al., 2007). Although our findings have highlighted an association between TGFβ-SMAD2/3 signalling and the phenotype of primordial GCs, further studies will be required to elucidate the molecular link between this pathway and regulation of the cell cycle.

We have also shown that, reciprocally, a significant proportion of GCs lacking nuclear SMAD2/3 are undergoing proliferation, as indicated by the proliferation marker Ki67. Modulation of TGFβ signalling can occur through ligand availability, expression of receptors and co-receptors, internal antagonism of SMADs and SMAD-independent pathways, as well as interaction or availability of transcriptional co-factors (Massagué, 2012; Wakefield and Hill, 2013). Since growing preantral follicles are known to express a

Journal of Cell Science (2018) 131, jcs218123. doi:10.1242/jcs.218123

range of extracellular antagonists, including follistatin, HTRA1, TWSG1, CTGF and GREM2 (Fenwick et al., 2011; Harlow et al., 2002; Shimasaki et al., 1989), it is plausible these proteins could act on neighbouring follicles to inhibit TGFβ signalling in this context. Indeed, direct inhibition of the Type I TGFβ receptors *in vitro* leads to increased follicle activation in neonatal mouse ovaries (Wang et al., 2014). We have also demonstrated that modulation of serine-threonine kinase receptor associated protein (STRAP), can affect early follicle development (Sharum et al., 2017), presumably through known interactions that influence downstream SMAD2/3 signalling (Datta and Moses, 2000). Thus, there are multiple mechanisms that can potentiate the observed change in SMAD2/3 signalling in early growing follicles.

On the other hand, exclusion of SMAD2/3 from GC nuclei of early growing follicles is slightly paradoxical, since this coincides with increased expression of GDF9 in oocytes, a TGFβ ligand that acts on GCs to promote proliferation (Elvin et al., 1999; Hayashi et al., 1999; Vitt et al., 2000). TGFβ signalling is known to be context dependent (Massagué, 2012); for example, in endothelial cells, exposure to low levels of TGFβ supports a SMAD2/3-dependent cytostatic phenotype, whereas elevated levels initiate a change to a SMAD1/5/8-mediated proliferative phenotype (Goumans et al., 2002). Whether a similar mechanism exists in quiescent versus proliferating GCs is not known; however, it is interesting to note that the reduction in nuclear SMAD2/3 in growing follicles coincides with an increase in SMAD1/5/8 expression in GCs (Fenwick et al., 2013; Sharum et al., 2017). Moreover, in cultured human biopsies, activin A, which signals via SMAD2/3, was found to inhibit or promote activation of primordial follicles depending on the concentration of the ligand (Ding et al., 2010). Increased exposure to certain TGFβ ligands may therefore initiate a change in the way GCs respond to TGFβ signalling. Importantly, TGFβ ligand-receptor complexes can also drive SMAD-independent pathways, including PI3K/AKT, mTOR and MAPK (Lamouille et al., 2012; Lamouille and Derynck, 2007; Lee et al., 2007). Activation of PI3K/AKT and mTOR pathways both promote early follicle growth in mice (Castrillon et al., 2003; Liu et al., 2007a, b; Zhang et al., 2014). The findings presented here suggest stage-dependent responses to TGFβ signalling in GCs.

Proliferating GCs of early growing follicles express a range of growth factors capable of regulating oocyte growth via the PI3K pathway (Adhikari and Liu, 2009; Thomas and Vanderhyden, 2006). Activation of the PI3K pathway leads to phosphorylation and nuclear exclusion of FOXO3 in these cells, which is a key molecular indicator of growth (Castrillon et al., 2003; Liu et al., 2007a). Based on our findings, it is likely that GCs proliferate and change shape prior to oocyte growth. The earliest molecular events that control these morphological changes are likely to be regulated by TGFβ signals in GCs as proposed (Fig. 7). This raises a number of questions in terms of identifying the specific TGFβ factor(s) that act on primordial GCs, the downstream targets of SMAD2/3, and the molecular events that precipitate SMAD2/3 nuclear exclusion. Clarifying these details would potentially provide a new framework for improving our understanding of how the ovarian reserve is maintained and how some follicles are activated to grow.

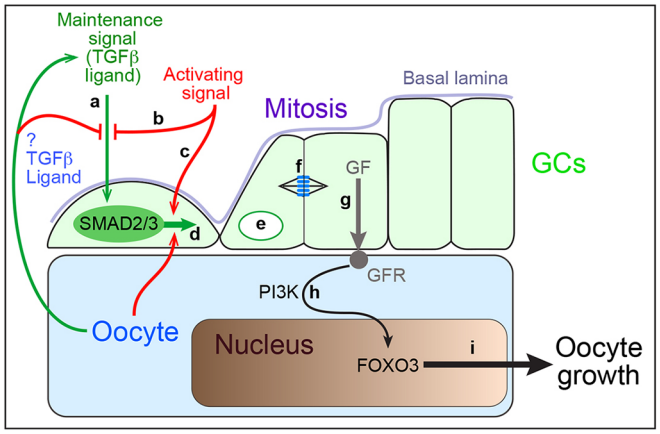

Fig. 7. Proposed model for activation of follicle growth. GCs of primordial follicles receive a TGFβ signal from the external environment or the oocyte that maintains active SMAD2/3 in GC nuclei (a) and inhibits GC proliferation. An activation signal (red arrows; b,c), whose source and identity remains unknown, can either be an inhibitor of the maintenance ligand (b) or a factor that acts on the nucleus directly, dephosphorylating SMAD2/3 (c), resulting in export of SMAD2/3 from the nucleus (d). Export of SMAD2/3 from the nucleus (e) removes the cell cycle inhibition, resulting in GC proliferation (f), which in turn causes GCs to become more tightly packed. A growth factor (GF) of unknown identity, which is increasingly expressed as GCs cuboidalize and proliferate, will interact with its receptor (GFR) on the oocyte surface (g), with PI3K signalling (h) resulting in the export of the transcription factor FOXO3 (i) from the oocyte nucleus, and oocyte growth.

MATERIALS AND METHODS

Ovary collection, culture and immunohistochemistry

C57BL/6 female mice were housed in accordance with the Animals (Scientific Procedures) Act of 1986 and associated Codes of Practice. Ovaries were dissected from mice at 4 and 12 days post-partum (d4 pp; d12 pp), at which stages they contain a preponderance of primordial and early growing follicles, respectively (Fenwick et al., 2011; Kerr et al., 2006; Sharum et al., 2017). In the d12 mouse ovary, somatic cells from growing follicles are proposed to originate from an initial developmental wave, which eventually contributes to fertility during the first three months after puberty, whereas somatic cells from primordial follicles contribute to fertility after this (Mork et al., 2012; Zheng et al., 2014). Given these distinct developmental origins, some analyses were also carried out on adult ovaries for comparison (Fig. S3). Ovaries were fixed in 10% neutral buffered formalin (NBF; 48 h) for later paraffin embedding and serial sectioning. Sections (5 µm) of ovary were dewaxed and rehydrated. Antigen retrieval was performed by boiling slides in citrate buffer (10 mmol l^{-1} citric acid; pH 6.0; 4×5 min) or Tris buffer (100 mmol l^{-1}, pH 10.0) with 5% (w/v) urea and non-specific binding blocked using 10% (v/v) goat serum (Invitrogen, ThermoFisher, UK) with 4% (w/v) BSA (Sigma-Aldrich, Poole, UK). Primary antibodies were applied overnight at 4°C. Primary antibodies used were rabbit anti-MVH (3 µg ml^{-1}; ab13840, Abcam, Cambridge, UK); rabbit anti-laminin (2.7 µg ml^{-1}; ab11575, Abcam); mouse monoclonal anti-SMAD 2/3 (0.25 µg ml^{-1}; 133098, Santa Cruz Biotechnology); rabbit polyclonal anti-Ki67 (1:200; ab15580, Abcam); rabbit monoclonal anti-MCM2 (3619 Cell Signaling). After washes in PBS, sections were incubated in an appropriate Alexa Fluor™ fluorescently labelled secondary antibody (1:200; Invitrogen) for 40 min. All sections were mounted in Prolong Gold medium containing 4,6-diamino-2-phenylindole (DAPI, Invitrogen). Labelling of rabbit monoclonal anti-FOXO3a (1:200; 2497; Cell Signalling Technology) was visualized with a peroxidase-conjugated avidin biotin complex (ABC kit; Vector Labs, Peterborough, UK) and 3,3′-diaminobenzidine tetrahydrochloride (DAB brown kit; Invitrogen). Granulosa cell proliferation was assessed using a PCNA staining kit, with a DAB detection system (93-1143; Zymed; Thermo Fisher, UK) according to the manufacturer's instructions.

Transmission electron microscopy

Ovaries were fixed for 24 h in 3% v/v glutaraldehyde in 0.1 mol l^{-1} cacodylate buffer (pH 7.2), post-fixed in 1% osmium tetroxide in cacodylate buffer for 1 h and embedded in Epon (TAAB Laboratories Equipment Ltd). Ultrathin sections were stained in a saturated solution of uranyl acetate in 50% ethanol, followed by Reynold's lead citrate, and examined using a Tecnai Spirit (FEI) electron microscope.

Scoring follicle stage

The stage of follicle development was assessed on the basis of granulosa cell shape. Primordial follicles were enveloped by a single layer of flattened GCs; zip follicles had two wedged-shaped GCs abutting each other, with or without adjacent flat GCs; transitional follicles had a mixture of flattened and cuboidal GCs surrounding the oocyte; primary follicles were surrounded by a complete layer of cuboidal GCs and primary+ follicles were developing a second layer of one or more GCs adjacent to the oocyte.

Image acquisition and analysis

For all studies, digital images were taken encompassing two or three entire ovary sections from three ovaries. For DAB-stained sections, images were acquired with a DS-Fi1 digital camera (Nikon, Kingston-upon-Thames, UK) attached to an E600 microscope (Nikon), using the NIS-Elements AR image analysis program (version 3.10; Nikon). For immunofluorescence, RGB images were acquired using a Leica inverted SP5 confocal laser-scanning microscope (Leica Microsystems, Wetzlar, Germany) with a ×40 oil immersion objective. A single image of the entire section was compiled from individual images using DoubleTake (Version 2.2.8; http://echoone.com/doubletake/). This allowed the numbering of individual follicles for analysis, ensuring that follicles were not measured twice or omitted. Original high-power DAB-stained or RGB images were analysed using ImageJ (http://imagej.nih.gov/ij), with reference to the annotated, compiled whole-ovary section image. Images were calibrated to pixels/μm. Using 'Measure and Label' in ImageJ, each measurement (whether follicle, oocyte or individual GC) was numbered on the image, allowing data to be matched to images.

SMAD2/3 and Ki67 expression was quantified by analysing confocal RGB images that had been separated into individual 8-bit greyscale images. In the relevant channel for the specific antibody, a threshold was set by adjusting the channel threshold until the degree of labelling visually matched that seen in the original image. This threshold was then maintained for analysis of the whole section. The area of positive pixels that exceeded this threshold was measured using ImageJ and presented as a proportion of the area of the structure in question, whether a nucleus or a sampling circle. For simplicity, we refer to this measure as 'intensity'. Light micrographs of FOXO3A immunohistochemistry (where DAB was used to visualize immunoreactivity and haematoxylin to visualize nuclei) were analysed using ImageJ. Images were viewed as 8-bit greyscale images and calibrated using intensity values from lightest and darkest nuclei. This calibration was maintained throughout the analysis. Images of haematoxylin staining alone were also analysed.

Data handling and analysis

ImageJ measurements and cropped images of individual follicles with ImageJ annotations were imported into custom-built databases (Filemaker Pro). This also allowed automatic calculation of follicle and oocyte diameter (d) ($2\times\sqrt{\text{area}/\pi}$), oocyte circumference (πd), and mean GC height [(Follicle diameter−oocyte diameter)/2]. Scoring of follicle stage (Fig. 1), GC shape and number of GC nuclei could be carried out within the database from the imported images. This simplified scoring and reduced operator error during data transcription. Statistical comparisons were carried out using Prism 6 for Mac OSX (www.graphpad.com). Data were generally non-normally distributed, so non-parametric analyses were used as stated in figure legends (Kruskal-Wallis test with a Dunn's post test).

Acknowledgements

The authors would also like to acknowledge Norah Spears (University of Edinburgh) and Sofia Granados Aparici (University of Sheffield) for useful discussion.

Competing interests

The authors declare no competing or financial interests.

Author contributions

Conceptualization: K.H., S.F., M.A.F.; Methodology: K.H., J.M.M., C.D., M.A.F.; Validation: K.H.; Formal analysis: K.H., C.D.; Investigation: K.H., J.M.M., C.D., R.C., M.A.F.; Resources: C.D.; Data curation: K.H.; Writing - original draft: K.H., M.A.F.; Writing - review & editing: K.H., S.F., M.A.F.; Visualization: K.H.; Supervision: K.H., S.F., M.A.F.; Project administration: K.H.; Funding acquisition: K.H., S.F., M.A.F.

Funding

This work was supported by grants received from the Biotechnology and Biological Sciences Research Council (BBSRC) UK awarded to K.H., S.F. and M.A.F. (BB/H00002X/1), the Medical Research Council (MRC) UK awarded to S.F. and K.H. (G0802782) and the Genesis Research Trust (UK).

Supplementary information

Supplementary information available online at
http://jcs.biologists.org/lookup/doi/10.1242/jcs.218123.supplemental

References

Adhikari, D. and Liu, K. (2009). Molecular mechanisms underlying the activation of mammalian primordial follicles. *Endocr. Rev.* **30**, 438-464.

Adhikari, D., Flohr, G., Gorre, N., Shen, Y., Yang, H., Lundin, E., Lan, Z., Gambello, M. J. and Liu, K. (2009). Disruption of Tsc2 in oocytes leads to overactivation of the entire pool of primordial follicles. *Mol. Hum. Reprod.* **15**, 765-770.

Adhikari, D., Zheng, W., Shen, Y., Gorre, N., Hamalainen, T., Cooney, A. J., Huhtaniemi, I., Lan, Z.-J. and Liu, K. (2010). Tsc/mTORC1 signaling in oocytes governs the quiescence and activation of primordial follicles. *Hum. Mol. Genet.* **19**, 397-410.

Andl, C. D. and Rustgi, A. K. (2005). No one-way street: cross-talk between e-cadherin and receptor tyrosine kinase (RTK) signaling: a mechanism to regulate RTK activity. *Cancer Biol. Ther.* **4**, 28-31.

Billiar, R. B., St Clair, J. B., Zachos, N. C., Burch, M. G., Albrecht, E. D. and Pepe, G. J. (2004). Localization and developmental expression of the activin signal transduction proteins Smads 2, 3, and 4 in the baboon fetal ovary. *Biol. Reprod.* **70**, 586-592.

Bravo, R. and Macdonald-Bravo, H. (1987). Existence of two populations of cyclin/proliferating cell nuclear antigen during the cell cycle: association with DNA replication sites. *J. Cell Biol.* **105**, 1549-1554.

Braw-Tal, R. (2002). The initiation of follicle growth: the oocyte or the somatic cells? *Mol. Cell. Endocrinol.* **187**, 11-18.

Castrillon, D. H., Miao, L., Kollipara, R., Horner, J. W. and DePinho, R. A. (2003). Suppression of ovarian follicle activation in mice by the transcription factor Foxo3a. *Science* **301**, 215-218.

Chen, C.-R., Kang, Y., Siegel, P. M. and Massagué, J. (2002). E2F4/5 and p107 as Smad cofactors linking the TGFbeta receptor to c-myc repression. *Cell* **110**, 19-32.

Choi, Y., Yuan, D. and Rajkovic, A. (2008). Germ cell-specific transcriptional regulator sohlh2 is essential for early mouse folliculogenesis and oocyte-specific gene expression. *Biol. Reprod.* **79**, 1176-1182.

Da Silva-Buttkus, P., Jayasooriya, G. S., Mora, J. M., Mobberley, M., Ryder, T. A., Baithun, M., Stark, J., Franks, S. and Hardy, K. (2008). Effect of cell shape and packing density on granulosa cell proliferation and formation of multiple layers during early follicle development in the ovary. *J. Cell Sci.* **121**, 3890-3900.

Da Silva-Buttkus, P., Marcelli, G., Franks, S., Stark, J. and Hardy, K. (2009). Inferring biological mechanisms from spatial analysis: prediction of a local inhibitor in the ovary. *Proc. Natl. Acad. Sci. USA* **106**, 456-461.

Datta, P. K. and Moses, H. L. (2000). STRAP and Smad7 synergize in the inhibition of transforming growth factor beta signaling. *Mol. Cell. Biol.* **20**, 3157-3167.

Ding, C. C., Thong, K. J., Krishna, A. and Telfer, E. E. (2010). Activin A inhibits activation of human primordial follicles in vitro. *J. Assist. Reprod. Genet.* **27**, 141-147.

Drummond, A. E., Le, M. T., Ethier, J.-F., Dyson, M. and Findlay, J. K. (2002). Expression and localization of activin receptors, Smads, and beta glycan to the postnatal rat ovary. *Endocrinology* **143**, 1423-1433.

Edson, M. A., Nagaraja, A. K. and Matzuk, M. M. (2009). The mammalian ovary from genesis to revelation. *Endocr. Rev.* **30**, 624-712.

Elvin, J. A., Yan, C., Wang, P., Nishimori, K. and Matzuk, M. M. (1999). Molecular characterization of the follicle defects in the growth differentiation factor 9-deficient ovary. *Mol. Endocrinol.* **13**, 1018-1034.

Erez, N., Bershadsky, A. and Geiger, B. (2005). Signaling from adherens-type junctions. *Eur. J. Cell Biol.* **84**, 235-244.

Fenwick, M. A., Mansour, Y. T., Franks, S. and Hardy, K. (2011). Identification and regulation of bone morphogenetic protein antagonists associated with preantral follicle development in the ovary. *Endocrinology* **152**, 3515-3526.

Fenwick, M. A., Mora, J. M., Mansour, Y. T., Baithun, C., Franks, S. and Hardy, K. (2013). Investigations of TGF-beta signaling in preantral follicles of female mice reveal differential roles for bone morphogenetic protein 15. *Endocrinology* **154**, 3423-3436.

Frederick, J. P., Liberati, N. T., Waddell, D. S., Shi, Y. and Wang, X.-F. (2004). Transforming growth factor beta-mediated transcriptional repression of c-myc is dependent on direct binding of Smad3 to a novel repressive Smad binding element. *Mol. Cell. Biol.* **24**, 2546-2559.

Gougeon, A. and Busso, D. (2000). Morphologic and functional determinants of primordial and primary follicles in the monkey ovary. *Mol. Cell. Endocrinol.* **163**, 33-42.
Goumans, M.-J., Valdimarsdottir, G., Itoh, S., Rosendahl, A., Sideras, P. and ten Dijke, P. (2002). Balancing the activation state of the endothelium via two distinct TGF-beta type I receptors. *EMBO J.* **21**, 1743-1753.
Hannon, G. J. and Beach, D. (1994). p15INK4B is a potential effector of TGF-beta-induced cell cycle arrest. *Nature* **371**, 257-261.
Harlow, C. R., Davidson, L., Burns, K. H., Yan, C., Matzuk, M. M. and Hillier, S. G. (2002). FSH and TGF-beta superfamily members regulate granulosa cell connective tissue growth factor gene expression in vitro and in vivo. *Endocrinology* **143**, 3316-3325.
Hayashi, M., McGee, E. A., Min, G., Klein, C., Rose, U. M., van Duin, M. and Hsueh, A. J. W. (1999). Recombinant growth differentiation factor-9 (GDF-9) enhances growth and differentiation of cultured early ovarian follicles. *Endocrinology* **140**, 1236-1244.
Herrera, L., Ottolenghi, C., Garcia-Ortiz, J. E., Pellegrini, M., Manini, F., Ko, M. S. H., Nagaraja, R., Forabosco, A. and Schlessinger, D. (2005). Mouse ovary developmental RNA and protein markers from gene expression profiling. *Dev. Biol.* **279**, 271-290.
Hikabe, O., Hamazaki, N., Nagamatsu, G., Obata, Y., Hirao, Y., Hamada, N., Shimamoto, S., Imamura, T., Nakashima, K., Saitou, M. et al. (2016). Reconstitution in vitro of the entire cycle of the mouse female germ line. *Nature* **539**, 299-303.
Hill, C. S. (2009). Nucleocytoplasmic shuttling of Smad proteins. *Cell Res.* **19**, 36-46.
Hirshfield, A. N. (1991). Development of follicles in the mammalian ovary. *Int. Rev. Cytol.* **124**, 43-101.
Hosaka, T., Biggs, W. H., III, Tieu, D., Boyer, A. D., Varki, N. M., Cavenee, W. K. and Arden, K. C. (2004). Disruption of forkhead transcription factor (FOXO) family members in mice reveals their functional diversification. *Proc. Natl. Acad. Sci. USA* **101**, 2975-2980.
Hutt, K. J., McLaughlin, E. A. and Holland, M. K. (2006). KIT/KIT ligand in mammalian oogenesis and folliculogenesis: roles in rabbit and murine ovarian follicle activation and oocyte growth. *Biol. Reprod.* **75**, 421-433.
John, G. B., Gallardo, T. D., Shirley, L. J. and Castrillon, D. H. (2008). Foxo3 is a PI3K-dependent molecular switch controlling the initiation of oocyte growth. *Dev. Biol.* **321**, 197-204.
Kerr, J. B., Duckett, R., Myers, M., Britt, K. L., Mladenovska, T. and Findlay, J. K. (2006). Quantification of healthy follicles in the neonatal and adult mouse ovary: evidence for maintenance of primordial follicle supply. *Reproduction* **132**, 95-109.
Knight, P. G. and Glister, C. (2006). TGF-beta superfamily members and ovarian follicle development. *Reproduction* **132**, 191-206.
Lamouille, S. and Derynck, R. (2007). Cell size and invasion in TGF-beta-induced epithelial to mesenchymal transition is regulated by activation of the mTOR pathway. *J. Cell Biol.* **178**, 437-451.
Lamouille, S., Connolly, E., Smyth, J. W., Akhurst, R. J. and Derynck, R. (2012). TGF-beta-induced activation of mTOR complex 2 drives epithelial-mesenchymal transition and cell invasion. *J. Cell Sci.* **125**, 1259-1273.
Lecanda, J., Ganapathy, V., D'Aquino-Ardalan, C., Evans, B., Cadacio, C., Ayala, A. and Gold, L. I. (2009). TGFbeta prevents proteasomal degradation of the cyclin-dependent kinase inhibitor p27kip1 for cell cycle arrest. *Cell Cycle* **8**, 742-756.
Lee, M. K., Pardoux, C., Hall, M. C., Lee, P. S., Warburton, D., Qing, J., Smith, S. M. and Derynck, R. (2007). TGF-beta activates Erk MAP kinase signalling through direct phosphorylation of ShcA. *EMBO J.* **26**, 3957-3967.
Lintern-Moore, S. and Moore, G. P. M. (1979). The initiation of follicle and oocyte growth in the mouse ovary. *Biol. Reprod.* **20**, 773-778.
Liu, H. C., He, Z. and Rosenwaks, Z. (2001). Application of complementary DNA microarray (DNA chip) technology in the study of gene expression profiles during folliculogenesis. *Fertil. Steril.* **75**, 947-955.
Liu, K., Rajareddy, S., Liu, L., Jagarlamudi, K., Boman, K., Selstam, G. and Reddy, P. (2006). Control of mammalian oocyte growth and early follicular development by the oocyte PI3 kinase pathway: new roles for an old timer. *Dev. Biol.* **299**, 1-11.
Liu, L., Rajareddy, S., Reddy, P., Du, C., Jagarlamudi, K., Shen, Y., Gunnarsson, D., Selstam, G., Boman, K. and Liu, K. (2007a). Infertility caused by retardation of follicular development in mice with oocyte-specific expression of Foxo3a. *Development* **134**, 199-209.
Liu, L., Rajareddy, S., Reddy, P., Jagarlamudi, K., Du, C., Shen, Y., Guo, Y., Boman, K., Lundin, E., Ottander, U. et al. (2007b). Phosphorylation and inactivation of glycogen synthase kinase-3 by soluble kit ligand in mouse oocytes during early follicular development. *J. Mol. Endocrinol.* **38**, 137-146.
Lundy, T., Smith, P., O'Connell, A., Hudson, N. L. and McNatty, K. P. (1999). Populations of granulosa cells in small follicles of the sheep ovary. *J. Reprod. Fertil.* **115**, 251-262.
Massagué, J. (2012). TGFbeta signalling in context. *Nat. Rev. Mol. Cell Biol.* **13**, 616-630.
McGee, E. A. and Hsueh, A. J. (2000). Initial and cyclic recruitment of ovarian follicles. *Endocr. Rev.* **21**, 200-214.
McLaughlin, E. A. and McIver, S. C. (2009). Awakening the oocyte: controlling primordial follicle development. *Reproduction* **137**, 1-11.
Mora, J. M., Fenwick, M. A., Castle, L., Baithun, M., Ryder, T. A., Mobberley, M., Carzaniga, R., Franks, S. and Hardy, K. (2012). Characterization and significance of adhesion and junction-related proteins in mouse ovarian follicles. *Biol. Reprod.* **86**, 153, 1–14.
Mork, L., Maatouk, D. M., McMahon, J. A., Guo, J. J., Zhang, P., McMahon, A. P. and Capel, B. (2012). Temporal differences in granulosa cell specification in the ovary reflect distinct follicle fates in mice. *Biol. Reprod.* **86**, 37.
Nilsson, E. E. and Skinner, M. K. (2004). Kit ligand and basic fibroblast growth factor interactions in the induction of ovarian primordial to primary follicle transition. *Mol. Cell. Endocrinol.* **214**, 19-25.
Oktay, K., Schenken, R. S. and Nelson, J. F. (1995). Proliferating cell nuclear antigen marks the initiation of follicular growth in the rat. *Biol. Reprod.* **53**, 295-301.
Packer, A. I., Hsu, Y. C., Besmer, P. and Bachvarova, R. F. (1994). The ligand of the c-kit receptor promotes oocyte growth. *Dev. Biol.* **161**, 194-205.
Pangas, S. A. (2012a). Bone morphogenetic protein signaling transcription factor (SMAD) function in granulosa cells. *Mol. Cell. Endocrinol.* **356**, 40-47.
Pangas, S. A. (2012b). Regulation of the ovarian reserve by members of the transforming growth factor beta family. *Mol. Reprod. Dev.* **79**, 666-679.
Pangas, S. A., Choi, Y., Ballow, D. J., Zhao, Y., Westphal, H., Matzuk, M. M. and Rajkovic, A. (2006). Oogenesis requires germ cell-specific transcriptional regulators Sohlh1 and Lhx8. *Proc. Natl. Acad. Sci. USA* **103**, 8090-8095.
Parrott, J. A. and Skinner, M. K. (1999). Kit-ligand/stem cell factor induces primordial follicle development and initiates folliculogenesis. *Endocrinology* **140**, 4262-4271.
Picton, H. M. (2001). Activation of follicle development: the primordial follicle. *Theriogenology* **55**, 1193-1210.
Rajareddy, S., Reddy, P., Du, C., Liu, L., Jagarlamudi, K., Tang, W., Shen, Y., Berthet, C., Peng, S. L., Kaldis, P. et al. (2007). p27kip1 (cyclin-dependent kinase inhibitor 1B) controls ovarian development by suppressing follicle endowment and activation and promoting follicle atresia in mice. *Mol. Endocrinol.* **21**, 2189-2202.
Rajkovic, A., Pangas, S. A., Ballow, D., Suzumori, N. and Matzuk, M. M. (2004). NOBOX deficiency disrupts early folliculogenesis and oocyte-specific gene expression. *Science* **305**, 1157-1159.
Schmidt, D., Ovitt, C. E., Anlag, K., Fehsenfeld, S., Gredsted, L., Treier, A.-C. and Treier, M. (2004). The murine winged-helix transcription factor Foxl2 is required for granulosa cell differentiation and ovary maintenance. *Development* **131**, 933-942.
Scholzen, T. and Gerdes, J. (2000). The Ki-67 protein: from the known and the unknown. *J. Cell. Physiol.* **182**, 311-322.
Seoane, J., Pouponnot, C., Staller, P., Schader, M., Eilers, M. and Massagué, J. (2001). TGFbeta influences Myc, Miz-1 and Smad to control the CDK inhibitor p15INK4b. *Nat. Cell Biol.* **3**, 400-408.
Sharum, I. B., Granados-Aparici, S., Warrander, F. C., Tournant, F. P. and Fenwick, M. A. (2017). Serine threonine kinase receptor associated protein regulates early follicle development in the mouse ovary. *Reproduction* **153**, 221-231.
Shimasaki, S., Koga, M., Buscaglia, M. L., Simmons, D. M., Bicsak, T. A. and Ling, N. (1989). Follistatin gene expression in the ovary and extragonadal tissues. *Mol. Endocrinol.* **3**, 651-659.
Skinner, M. K. (2005). Regulation of primordial follicle assembly and development. *Hum. Reprod. Update* **11**, 461-471.
Stubbs, S. A., Stark, J., Dilworth, S. M., Franks, S. and Hardy, K. (2007). Abnormal preantral folliculogenesis in polycystic ovaries is associated with increased granulosa cell division. *J. Clin. Endocrinol. Metab.* **92**, 4418-4426.
Thomas, F. H. and Vanderhyden, B. C. (2006). Oocyte-granulosa cell interactions during mouse follicular development: regulation of kit ligand expression and its role in oocyte growth. *Reprod. Biol. Endocrinol.* **4**, 19.
Uda, M., Ottolenghi, C., Crisponi, L., Garcia, J. E., Deiana, M., Kimber, W., Forabosco, A., Cao, A., Schlessinger, D. and Pilia, G. (2004). Foxl2 disruption causes mouse ovarian failure by pervasive blockage of follicle development. *Hum. Mol. Genet.* **13**, 1171-1181.
Vitt, U. A., Hayashi, M., Klein, C. and Hsueh, A. J. W. (2000). Growth differentiation factor-9 stimulates proliferation but suppresses the follicle-stimulating hormone-induced differentiation of cultured granulosa cells from small antral and preovulatory rat follicles. *Biol. Reprod.* **62**, 370-377.
Wakefield, L. M. and Hill, C. S. (2013). Beyond TGFbeta: roles of other TGFbeta superfamily members in cancer. *Nat. Rev. Cancer* **13**, 328-341.
Wandji, S.-A., Sršeň, V., Voss, A. K., Eppig, J. J. and Fortune, J. E. (1996). Initiation in vitro of growth of bovine primordial follicles. *Biol. Reprod.* **55**, 942-948.
Wandji, S. A., Srsen, V., Nathanielsz, P. W., Eppig, J. J. and Fortune, J. E. (1997). Initiation of growth of baboon primordial follicles in vitro. *Hum. Reprod.* **12**, 1993-2001.
Wang, Z.-P., Mu, X.-Y., Guo, M., Wang, Y.-J., Teng, Z., Mao, G.-P., Niu, W.-B., Feng, L.-Z., Zhao, L.-H. and Xia, G.-L. (2014). Transforming growth factor-beta signaling participates in the maintenance of the primordial follicle pool in the mouse ovary. *J. Biol. Chem.* **289**, 8299-8311.

Journal of Cell Science (2018) 131, jcs218123. doi:10.1242/jcs.218123

Xu, J., Oakley, J. and McGee, E. A. (2002). Stage-specific expression of Smad2 and Smad3 during folliculogenesis. *Biol. Reprod.* **66**, 1571-1578.

Yang, J., Medvedev, S., Yu, J., Tang, L. C., Agno, J. E., Matzuk, M. M., Schultz, R. M. and Hecht, N. B. (2005). Absence of the DNA-/RNA-binding protein MSY2 results in male and female infertility. *Proc. Natl. Acad. Sci. USA* **102**, 5755-5760.

Zhang, H., Risal, S., Gorre, N., Busayavalasa, K., Li, X., Shen, Y., Bosbach, B., Brännström, M. and Liu, K. (2014). Somatic cells initiate primordial follicle activation and govern the development of dormant oocytes in mice. *Curr. Biol.* **24**, 2501-2508.

Zhang, Y., Alexander, P. B. and Wang, X. F. (2017). TGF-beta family signaling in the control of cell proliferation and survival. *Cold Spring Harb. Perspect. Biol.* **9**, 1-22.

Zheng, W., Zhang, H., Gorre, N., Risal, S., Shen, Y. and Liu, K. (2014). Two classes of ovarian primordial follicles exhibit distinct developmental dynamics and physiological functions. *Hum. Mol. Genet.* **23**, 920-928.